First astronomical results from the ARGO-YBJ detector

Carlo Ferrigno
INAF/IASF Palermo
and INFN Sezione di Catania
via Ugo La Malfa, 153
Palermo, Italy I-90146
Email: ferrigno@ifc.inaf.it

for the ARGO-YBJ collaboration

***Abstract*— ARGO-YBJ is an air shower detector made by a continuous carpet of resistive plate counters with an area of $\sim 7000\,\mathrm{m}^2$, located in Tibet (China) at 4300 m a.s.l. The aim of the experiment is to study cosmic rays and γ-radiation with an energy threshold of a few hundreds of GeV. The large field of view and the high duty cycle typical of air shower experiments allow the continuous monitoring of a large part of the sky, in order to search for unknown gamma ray sources and transient emissions as flares of Active Galactic Nuclei and Gamma Ray Bursts. The detector setting-up will be completed within 2006. Its modularity allows however to take data also in a partial configuration. ARGO-YBJ is presently running, since February 2006, with $4500\,\mathrm{m}^2$ of equipped surface (70% of the full area). In this work we present our first observations of the Moon shadow obtained with a detector subset of $\sim 1900\,\mathrm{m}^2$ and a preliminary sky survey searching for γ-ray sources.**

I. Introduction

ARGO-YBJ is an experiment aiming at the detailed study of cosmic radiation physics in the energy range between a few hundreds of GeV to about 100 TeV. ARGO-YBJ distinctive features are:

- high altitude operation (4300 m a.s.l. at Yangbajing in Tibet);
- full coverage of the equipped area, since the detector consists of a carpet of Resistive Plate Chambers (RPCs), covering $6700\,\mathrm{m}^2$;
- high duty cycle, due to the adopted technique of recording the Extended Air Shower (EAS) secondary particles produced by the incoming primary.

The main physics issues addressed by ARGO-YBJ are:

- γ-ray astronomy in the energy range starting from a few hundreds of GeV up to tens of TeV. Its very large acceptance, coupled to the high duty cycle make ARGO-YBJ well suited for the search of new sources and for the detailed description of transient phenomena. The data presented in this paper refer mainly to the preliminary analysis performed to investigate this item, essentially cross-checking the expected performance of the detector with the experimental results;
- hadronic cosmic ray (CR) physics in the energy range 1-1000 TeV, overlapping the upper range of direct satellite measurements and the lower range of ground-based EAS sampling detectors. The preliminary results obtained with the same data used for the analysis presented in this paper can be found in [1];
- Gamma Ray Burst (GRB) physics. High energy (GeV-TeV range) counterpart of satellite observations can be searched for;
- Sun and heliosphere physics at an energy E $\geq$ 10 GeV. CR modulation studies, Forbush decreases observation, monitoring of interplanetary magnetic field and detection of high energy protons and neutrons (ground level enhancements) from solar flares can be performed. A discussion of this item can be found in [2].

The experiment has been conceived and is being realised by a wide collaboration of Chinese and Italian scientific institutions. This paper is organised as follows: in Sect. II we describe the detector lay-out, and in Sect. III the data used in this analysis. In Sect. IV, V, and VI we report the search for stable γ-ray sources, for the Moon shadow, and for Gamma Ray Bursts. Finally, in Sect. VII we draw our conclusions.

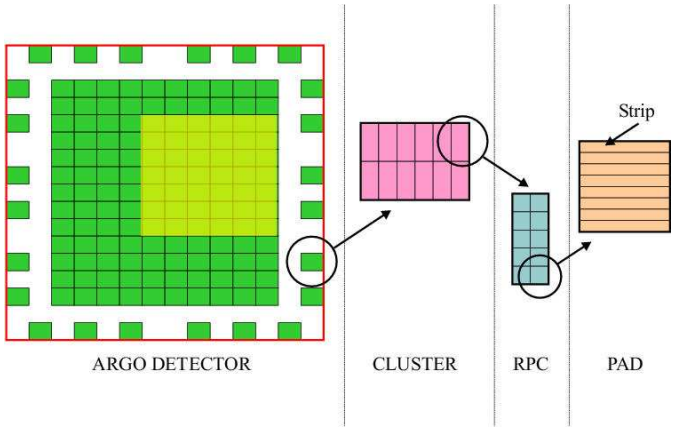

Fig. 1. The ARGO layout. The 42 clusters used in this preliminary analysis are shown in light yellow.

II. Detector lay-out

ARGO-YBJ is a modular detector, of the ground-based Extended Air Shower Detector (EASD) category. The detection modules are the RPC "clusters": 12 RPCs ($1.26 \times 2.85\,\mathrm{m}^2$) form a cluster. 130 adjacent clusters, disposed in 13 rows of 10 clusters each, constitute the ARGO central carpet ($74.5 \times 78\,\mathrm{m}^2$), whose main feature is the continuity: its active area is in fact 93%. As shown in Fig. 1, 24 external clusters surround the central carpet with a lower coverage (characterized by $\sim 40\%$ of active area), and act as a guard ring, helpful to enlarge the active area and to define contained events. Together with the central carpet, they define the detector, whose surface reaches $11\,000\,\mathrm{m}^2$ with $\sim 60\%$ overall coverage. The RPCs are filled with a gas mixture made by argon (15%), isobutane (10%), tetrafluorethane (75%). Ionizing particles produce electron streamers in the gas volume contained between two HV electrodes. The read-out is done through induction strips, $61.8 \times 6.75\,\mathrm{cm}^2$ wide, placed on one face of the chamber. There are 80 strips per chamber. They are the elementary digital read-out elements, whose dimension determines the ARGO spatial resolution. The characterisation of the shower front topology, essential to discriminate a hadronic from a photon primary, critically depends on this parameter, which has an importance also in the determination of the core position and the shower size, and hence of the energy dynamical range of the experiment.

The digital signals coming by 8 adjacent strips are OR-ed to build the PAD signal, sent to single TDC channels. 10 PADs per chamber allow to describe the time structure of the shower front in a detailed way. The RPC time resolution of about 1 ns and the detector calibration method contribute to determine the angular resolution of ARGO. The PAD signal is also used to trigger the data acquisition. The trigger modes are the so-called "scaler mode" just counting the number of fired PADS in a time window of 0.5 s within a single cluster, and the so-called "shower mode", where a majority logic is built, requiring a minimum number of fired PADS $N_{\mathrm{PAD}} > N_{\mathrm{th}}$, within a close time window coincidence of 400 ns. A relatively low threshold ($N_{\mathrm{th}} = 20$) selects low energy showers, whereas a high threshold ($N_{\mathrm{th}} = 60$) in the whole detector selects high energy showers. The scaler mode is intended mainly for testing purposes (the stability of the rate of fired PADS within a cluster is a rather good parameter for monitoring the "state of health" of the RPCs), as well as for GRB detection in the GeV energy range in correlation with satellite measurements, as it will be outlined in Sect. VI.

A detailed discussion of the detector performance can be found in [2], whereas a description of the ARGO RPC is given in [3].

The detector modularity allowed the data taking to start even during the setting up, as soon as a significant part of the detector was installed. From November 2003 to December 2004, 16 clusters were in place, and a first period of data taking has been performed, mainly for testing and debugging purposes, while other detector modules were up-loaded and set-up in place. From December 2004 to July 2005, 42 clusters, corresponding to ∼30% of the detector, have been operated for a first period of physics data taking. The preliminary results discussed in this paper refer to these data.

Since July 2006, 130 clusters, i.e. the full central carpet, were in place. ARGO-YBJ will start data taking in its full configuration, i.e. with 154 clusters, at the beginning of 2007. The set-up will be further upgraded during 2007 by the addition of a layer of lead 1 r.l. ($0.5\,\mathrm{cm}$) thick, to be used as photon converter, on top of the RPCs.

III. Data

The data used in this analysis have been recorded by a detector subset consisting of a $\sim 47 \times 41\ \mathrm{m}^2$ RPC carpet for an area of $\sim\ 1900\,\mathrm{m}^2$. The minimum number of fired pads N_{PAD} required to trigger the detector was 60. This temporary trigger configuration (used to debug the detector) corresponds to an energy threshold relatively high: according to simulations, given a γ-ray source with a power law spectrum of index $\alpha = 2.5$ (2.0) extending up to 50 TeV and zenith angle $\theta = 20^{\mathrm{o}}$, the median energy of the detected γ-rays is ~ 4 (~ 8) TeV.

The arrival direction of the primary particles has been reconstructed by fitting the shower front with a conical shape of slope $0.03\,\mathrm{ns\,m^{-1}}$. The position of the shower core has been calculated by means of the Maximun Likelihood Method applied to the lateral density profile of the shower [4].

According to simulations, the distribution of the angle α between the true direction and the reconstructed one is well described by a Gaussian distribution $\mathrm{d}N/\mathrm{d}\alpha \propto e^{-0.5\alpha^2/\sigma^2}\sin\alpha$, where the parameter σ is defined as the angular resolution. The classical cut with a circular window of semi-aperture $\psi_{70} = 1.58\sigma$ contains 71.5% of the source events and maximizes the signal to noise ratio.

The angular resolution depends on the number of fired pads: for $N_{\mathrm{PAD}} > 60$ and the ARGO-YBJ configuration with 42 clusters, a circular window around the source with a half opening angle $\psi_{70} = 1.5^{\mathrm{o}}$ contains $\sim$ 70% of the events induced by γ-rays of energy 1-10 TeV and zenith angle $\theta = 20^{\mathrm{o}}$.

The data set of this analysis was recorded from December 24, 2004 to July 17, 2005, for a total run time of 62.3 days. The event rate was $\sim$160 Hz. Since in this work we consider the events with zenith angle $\theta < 40^{\mathrm{o}}$, we are monitoring the declination band $-10^{\mathrm{o}} < \delta < 70^{\mathrm{o}}$, corresponding to 7.0 sr (55% of the celestial sphere). No gamma-hadron discrimination is performed on these preliminary data.

IV. Search for stable gamma-ray sources

The search for point gamma ray sources consists in filling a sky map with all the detected showers and comparing each bin content with the expected background due to cosmic rays. We divided the sky into bins of equal area exploiting the *H*ealpix library [5]. Then, taking into account the angular resolution of the detector in the 1-10 TeV energy range, we smoothed the image using a circular window of 3^{o} diameter. Since the position of possible sources is unknown we oversample the sky in order to detect a possible source near the edge of a bin. Each map contains a total of 200 000 non independent bins. The content of each bin N_s is compared with the expected background N_b. The background map has been built using a method similar to the "time swapping method" [6], randomly changing the time of each real event inside a time interval of a few hours, during which both the background and the response of the detector can be assumed to be constant. Each real event is used to generate 8 different background events, in order to increase the statistics of the background map.

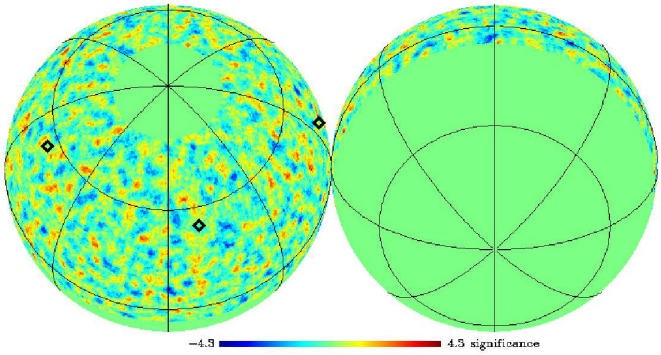

Fig. 2. Preliminary sky map obtained in 62.3 days of data taking. The three small diamonds indicate the positions of the Crab Nebula, Mrk 421 and Mrk 501 (from left to right).

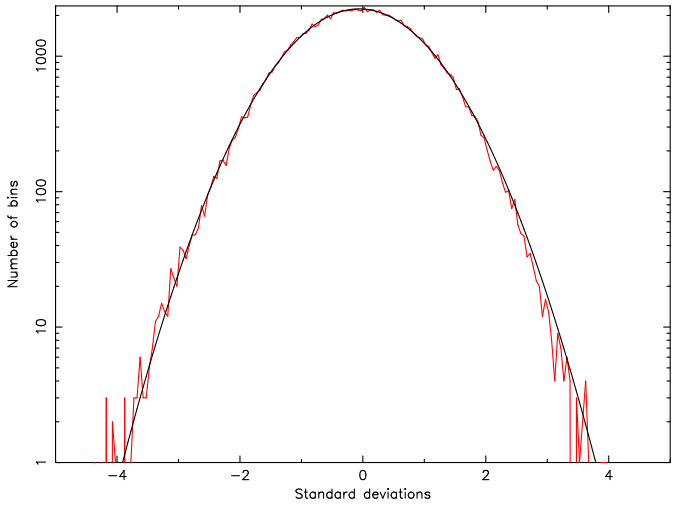

Fig. 3. Distribution of the excesses in the 200 000 bins of the sky map in unit of standard deviations, with a Gaussian fit overlapped.

Fig. 2 shows the sky map obtained with the whole set of data, corresponding to 7.6×10^8 events. For each bin the value of the variable $n_\sigma = (N_s - N_b)/\sqrt{N_b}$ is reported. The distribution of n_σ is well fitted by a Gaussian distribution with $\sigma = 1.02$ (see Fig. 3). No excess larger than 4.0σ is observed. Given the limited run time of the present data, the Crab Nebula is expected to give a signal of ~ 1 standard deviation.

The daily rate of events from this source has been evaluated by simulating a gamma ray flux on the top of the atmosphere according to the spectrum $\mathrm{d}N/\mathrm{d}E = 3.2 \times 10^{-7} E^{-2.49} \gamma\mathrm{m}^{-2}\mathrm{s}^{-1}\mathrm{TeV}^{-1}$, measured by the Whipple collaboration [7]. The gamma rays have been simulated at different zenith angles, following the daily path of the source in the sky. At the Yangbajing site (latitude = 30^{o}

N) the Crab Nebula culminates at zenith angle $\theta = 8.1^{o}$. We "followed" the source when it was at $\theta < 30^{o}$.

The showers development in the atmosphere has been simulated by means of the Corsika code [8]. The response of the detector has been studied by using a GEANT3-based code (ARGO-G[1]), that gives position and time of all the fired PADS for every shower hitting the detector.

Assuming a source with a Crab-like spectrum (i.e. spectral index $\alpha = 2.49$) at a declination $\delta = 30^{o}$, where ARGO-YBJ is most sensitive, the gamma ray flux corresponding to 4.0σ is $F_{4\sigma} \approx 4$ Crab units. The flux limit increases as the declination varies from 30^{o}, being $F_{4\sigma} \approx 7(\approx 6)$ Crabs at $\delta = 10^{o}(50^{o})$ and $F_{4\sigma} \approx 10(\approx 12)$ Crabs at $\delta = 0^{o}(60^{o})$.

V. Check of the Moon shadow profile

The observation of the Moon shadow by a ground-based EAS array is very useful to calibrate its performance. Because almost all primary cosmic rays are positively charged, they are bent westward by the geomagnetic field at Yangbajing, therefore, the position of the Moon shadow shifts from the true Moon location. On the other hand, they are unaffected in the north-south direction as the east-west component of the geomagnetic field is negligible at Yangbajing. Since the geomagnetic field between the Earth and the Moon is accurately measured and modeled, and both the spectrum and the composition of cosmic rays at energies$< 100\,$TeV are directly measured, the observed position and the shape of the Moon shadow can be used to calibrate the possible systematic error in the angular resolution. At the same time the absolute pointing (north-south direction) to the primary cosmic ray directions, resulting from the EAS event reconstruction procedure, can be accurately verified. In addition, the Moon (and Sun) shadows can be used as a tool to study the interplanetary magnetic field between the Sun and the Earth [9].

From the data described in Sect. III we selected the events matching the following criteria: a) the reconstructed core position is within the ARGO carpet; b) $\chi^2/\mathrm{N_{hit}} < 1$ where χ^2 is obtained from the conical fit to the shower front and $\mathrm{N_{hit}}$ is the number of detected particles; c)the zenith angle of the arrival direction should be less than 40^{o} . After these selections and quality cuts, 2.1×10^{8} events remain for further analysis. In order to extract a deficit in CR events coming from the Moon, the background event density must be carefully estimated. This is done by averaging over 6 off-source cells with the same size, at the same zenith angle, and recorded at the same time intervals as the on-source cell events. This method, so-called "equi-zenith angle background estimation" [10], can reliably estimate the background events under the same condition as on-source events. The Moon shadow which we found is shown in Fig. 4. Due to the oversampling with respect to the expected resolution, we smoothed the image using a circular top-hat filter of 1.5^{o} radius, corresponding to the ψ_{70} of the selected data [11]. The maximum significance (4.9σ) is found at 0.7^{o} west and 0.5^{o} north of the true Moon position.

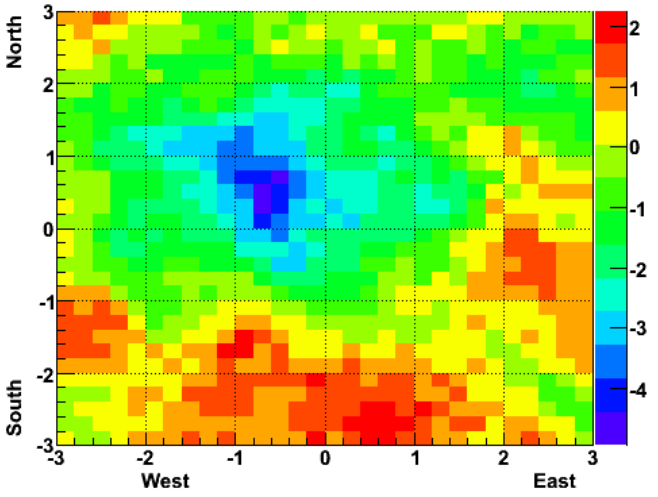

Fig. 4. Significance map in a $6^{o} \times 6^{o}$ square centred on the true Moon location. The colour scale is in standard deviations.

For a better understanding of the significance of our results, we developed a detailed MonteCarlo (MC) simulation of the Moon shadow assuming for the geomagnetic field the IGRF model [12] at altitudes below 600 km and the dipole model above 600 km (moment $M = 8.07 \times 10^{25}\,\mathrm{Gauss\,cm^3}$, south geomagnetic pole 78.3^{o} S, 111.0^{o} E). The relative chemical composition of primary cosmic rays was based mainly on direct observational data [13] using a heavy dominated model. The EAS events were simulated using the Corsika code [8] with QGSJET for the hadronic interaction model along the Moon orbit around the Earth. The secondary particles generated by the Corsika code are traced down to the Yangbajing site, and time and charge information of each particle is converted to ADC and TDC values by the detailed detector simulation code ARGO-G. Thus, we treat and analyse the MC events in the same way as the

[1]More information on the ARGO-G Monte-Carlo code can be found at the URL `http://argo.le.infn.it/analysis/argog/`

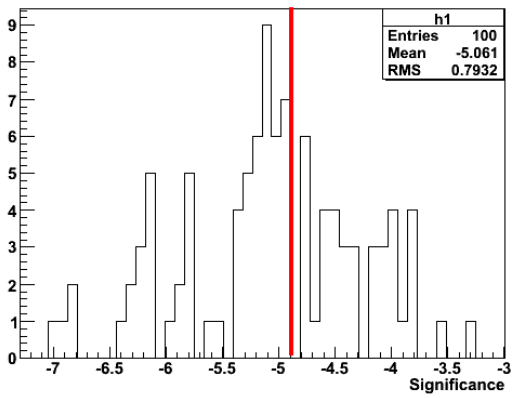

Fig. 5. Distribution of the maximum significance of the Moon deficit for 100 realizations of a MC simulation of the ARGO-YBJ observations. The vertical red line represents the deficit significance obtained from the data.

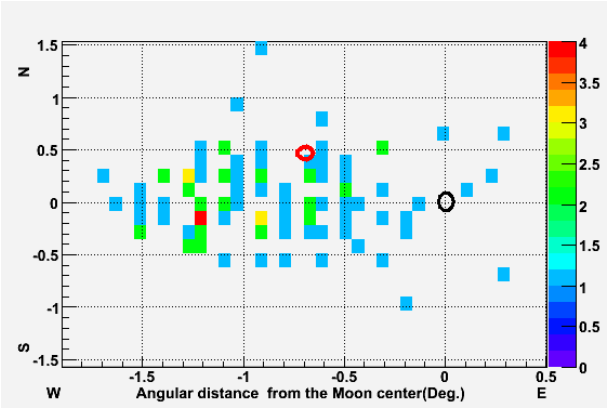

Fig. 6. Distribution of the Moon deficit displacement form the true Moon position for 100 realizations of a MC simulation of the ARGO-YBJ observations. East is on the right and North on the top, the axes are in degrees, the colour scale indicates the number of occurrences, the red circle is the measured deficit centroid and the black circle is the true Moon position.

experimental data.

In a second phase, a triggered primary gets a reverse charge sign and is shot back to the Moon, in a direction extracted according to the angular resolution found for ARGO-YBJ. A trajectory impinging on the Moon disk is therefore assigned to participate to a a positive Moon peak.

We made 100 realizations with the same number of events which match the selection criteria outlined for the real data, and found the distribution of the maximum deficit significance shown in Fig. 5 with a spread of positions shown in Fig. 6. The result obtained from the real data is consistent with the MC simulation of the available data set.

The cumulative deficit of the events coming from the Moon direction with respect to any other position is also a direct indication of the apparatus angular resolution. The deficit in a portion of the sky with angular area $S_{\rm off}$ including the Moon is:

$$\Delta N \simeq \eta \frac{S_{\rm Moon}}{S_{\rm off}} N_{\rm off} \qquad (1)$$

where $S_{\rm Moon}$ is the area of the Moon, $N_{\rm off}$ id the number of events in the off-source direction, and η is given for a Gaussian point spread function by:

$$\eta = 1 - \exp\left(-\frac{1}{2}\left[\frac{R_s}{\sigma}\right]^2\right) \qquad (2)$$

where R_s is the radius of the smoothing window and σ is the angular resolution. As shown in Fig. 7 the expected deficit for $\sigma \simeq 1^{\rm o}$ is consistent with the measured one.

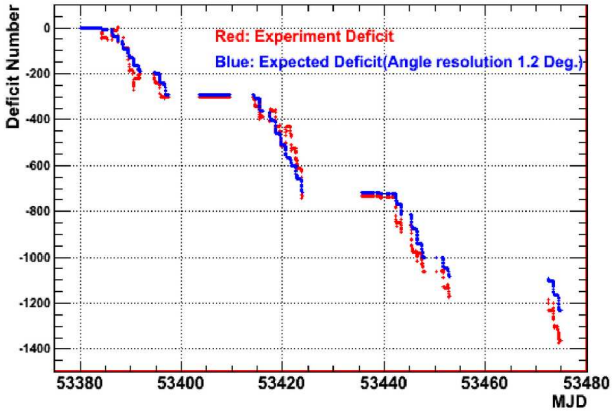

Fig. 7. Cumulative deficit of events from the Moon direction in the experimental data (red) and in the MC simulation (blue) for an angular resolution $\sigma \simeq 1^{\rm o}$.

VI. Search for Gamma Ray Bursts in scaler mode

GRBs at GeV energies can also be observed by ARGO under scaler mode. The GRB search is done in coincidence with satellite experiments, and started in correspondence with the first GRB detected by Swift on December 17, 2004. Data were collected with a detector area increasing from $\sim 700{\rm m}^2$ to $\sim 5600{\rm m}^2$. Up to August 2006, 32 GRBs detected by satellites were at a zenith angle $\theta < 40^{\rm o}$. Due to the detector installation and debugging, reliable data are available for only 19 of these GRBs [14].

In the scaler mode DAQ, for each cluster the signal

coming from the 120 pads is added up and put in coincidence in a narrow time window (150 ns), giving the rate of counts ≥ 1, ≥ 2, ≥ 3, ≥ 4, read by four independent scaler channels. For every GRB, the number of PAD counts N, recorded in each of the four multiplicity channels in the duration time $T90$ measured by the satellites, is compared with the number B of expected counts from the background (obtained from the average counting rate in $\pm 10 \cdot T90$ around the burst). The difference $N - B$ in units of standard deviations, $(N - B)/\sqrt{B + B/20}$, gives the statistical significance of the excess.

No convincing excess in the scaler counts was observed in the duration time measured by the satellites. The corresponding 3σ fluence upper limits in the 1-100 GeV energy range were estimated to be $10^{-4} \div 10^{-5}\,\mathrm{erg\,cm^{-2}}$, using the spectral indexes determined at the lower satellite energies. For those GRBs whose redshift is known, the upper limit was calculated including a simple $\gamma\gamma$ absorption model, while $z = 0$ was assumed for the others.

VII. Conclusions

The analysis of the first data taken by an ARGO-YBJ subset of area $\sim 1900\mathrm{m}^2$ shows that the detector is working properly.

- A preliminary sky survey searching for point sources shows no statistically significant excess during 62.3 days of measurement in the declination range $-10^{\mathrm{o}} < \delta < 70^{\mathrm{o}}$. In particular no source with an average flux larger than ~ 5 Crab units has been detected in the declination band $20^{\mathrm{o}} < \delta < 40^{\mathrm{o}}$ during this period.
- We detected the Moon shadow with 4.9σ significance at less than 1^{o} from the true position. This is consistent with the Monte-Carlo prediction for the angular resolution of $\sim 1^{\mathrm{o}}$ in the 1-10 TeV energy range.
- By means of scaler mode data collected with a detector area increasing from $\sim 700\mathrm{m}^2$ to $\sim 5600\mathrm{m}^2$, no significant emission from GRBs was detected up to now and fluence upper limits of $10^{-4} \div 10^{-5}\,\mathrm{erg\,cm^{-2}}$ in the 1-100 GeV energy range were obtained using the measured counting rates and GRB parameters determined by the satellite observations.

We expect for the final detector configuration (with an area more than 3 times larger and the lead converter layer) an improved angular resolution, a lower energy threshold and a significant increase in the gamma ray detection sensitivity.

References

[1] A. Surdo for the ARGO-YBJ collaboration, "Cosmic Ray phenomenology and measurement of the σ_{p-Air} with the ARGO-YBJ Experiment," in *these proceedings*, 2006.

[2] Z. Cao, "The Status of the ARGO Experiment in Tibet," in *International Cosmic Ray Conference*, 2005, p. 299.

[3] The ARGO-YBJ Collaboration, R. Assiro, C. Bacci, B. Bartoli, P. Bernardini, X. J. Bi, B. Biondo, C. Bleve, S. Bricola, F. Budano, S. Bussino, A. K. Calabrese Melcarne, P. Camarri, D. Campana, Z. Cao, R. Cardarelli, S. Catalanotti, S. Cavaliere, M. Cavalli Sforza, P. Celio, N. Cheng, P. Creti, G. Cusumano, B. Z. Dai, G. D'Alí Staiti, Danzengluobu, B. D'Aquino, E. De Marinis, I. De Mitri, B. D'Ettorre Piazzoli, M. De Vincenzi, T. Di Girolamo, X. H. Ding, G. Di Sciascio, C. F. Feng, Z. Feng, Z. Feng, K. Fratini, X. F. Gao, Q. B. Gou, H. H. He, M. He, H. Hu, H. Hu, Q. Huang, M. Iacovacci, I. James, H. Y. Jia, Labaciren, H. J. Li, J. Y. Li, B. Liberti, G. Liguori, C. Q. Liu, J. Liu, H. Lu, G. Mancarella, A. Mangano, S. M. Mari, G. Marsella, D. Martello, S. Mastroianni, X. R. Meng, J. Mu, L. Nicastro, C. C. Ning, M. Panareo, G. Pellizzoni, L. Perrone, C. Pino, C. Pinto, P. Pistilli, E. Reali, E. Rossi, L. Saggese, P. Salvini, R. Santonico, P. R. Shen, X. D. Sheng, F. Shi, C. Stanescu, A. Surdo, Y. H. Tan, P. Vallania, S. Vernetto, H. Wang, Y. Wang, Y. Wang, C. Y. Wu, H. R. Wu, L. Xue, H. T. Yang, Q. Y. Yang, X. C. Yang, G. C. Yu, A. F. Yuan, M. Zha, H. M. Zhang, J. L. Zhang, L. Zhang, N. J. Zhang, P. Zhang, X. Y. Zhang, Y. Zhang, Zhaxisangzhu, X. X. Zhou, F. R. Zhu, and Q. Q. Zhu, "Layout and performance of RPCs used in the Argo-YBJ experiment," *Nuclear Instruments and Methods in Physics Research A*, vol. 562, pp. 92–96, June 2006.

[4] G. Di Sciascio, C. Bleve, T. Di Girolamo, D. Martello, and E. Rossi for the ARGO-YBJ collaboration, "Identification of showers with cores outside the ARGO-YBJ detector," in *28th International Cosmic Ray Conference*, 2003, p. 3015.

[5] K. M. Górski, E. Hivon, A. J. Banday, B. D. Wandelt, F. K. Hansen, M. Reinecke, and M. Bartelmann, "HEALPix: A Framework for High-Resolution Discretization and Fast Analysis of Data Distributed on the Sphere," *ApJ*, vol. 622, pp. 759–771, Apr. 2005.

[6] D. E. Alexandreas, D. Berley, S. Biller, G. M. Dion, J. A. Goodman, T. J. Haines, C. M. Hoffman, E. Horch, X.-Q. Lu, C. Sinnis, G. B. Yodh, and W. Zhang, "Point source search techniques in ultra high energy gamma ray astronomy," *Nuclear Instruments and Methods in Physics Research A*, vol. 328, pp. 570–577, May 1993.

[7] A. M. Hillas, C. W. Akerlof, S. D. Biller, J. H. Buckley, D. A. Carter-Lewis, M. Catanese, M. F. Cawley, D. J. Fegan, J. P. Finley, J. A. Gaidos, F. Krennrich, R. C. Lamb, M. J. Lang, G. Mohanty, M. Punch, P. T. Reynolds, A. J. Rodgers, H. J. Rose, A. C. Rovero, M. S. Schubnell, G. H. Sembroski, G. Vacanti, T. C. Weekes, M. West, and J. Zweerink, "The Spectrum of TeV Gamma Rays from the Crab Nebula," *ApJ*, vol. 503, p. 744, Aug. 1998.

[8] D. Heck, J. Knapp, J. N. Capdevielle, G. Schatz, and T. Thouw, *CORSIKA: A Monte Carlo Code to Simulate Extensive Air Showers*, fzka report no. 6019, forschungszentrum karlsruhe ed., 1998.

[9] M. Amenomori, S. Ayabe, Caidong, Danzengluobu, L. K. Ding, Z. Y. Feng, Y. Fu, H. W. Guo, M. He, K. Hibino, N. Hotta, Q. Huang, A. X. Huo, K. Izu, H. Y. Jia, F. Kajino, K. Kasahara, Y. Katayose, Labaciren, J. Y. Li, H. Lu, S. L. Lu, G. X. Luo, X. R. Meng, K. Mizutani, J. Mu, H. Nanjo, M. Nishizawa, M. Ohnishi, I. Ohta, T. Ouchi, Z. R. Peng, J. R. Ren, T. Saito, M. Sakata, T. Sasaki, Z. Z. Shi, M. Shibata, A. Shiomi, T. Shirai, Y. Suga, H. Sugimoto, K. Taira, Y. H. Tan, N. Tateyama, S. Torii, T. Utsugi, C. R. Wang, H. Wang, X. W. Xu, Y. Yamamoto, G. C. Yu, A. F. Yuan, T. Yuda, C. S. Zhang, H. M. Zhang, J. L. Zhang, N. J. Zhang, X. Y. Zhang, Zhaxiciren, and Zhaxisangzhu, "A Study of the Shadowing of Galactic Cosmic Rays by the Sun in a Quiet Phase of Solar Activity with the Tibet Air Shower Array," *ApJ*, vol. 541, pp. 1051–1058, Oct. 2000.

[10] M. Amenomori, S. Ayabe, S. W. Cui, Danzengluobu, L. K. Ding, X. H. Ding, C. F. Feng, Z. Y. Feng, X. Y. Gao, Q. X. Geng, H. W. Guo, H. H. He, M. He, K. Hibino, N. Hotta, H. Hu, H. B. Hu, J. Huang, Q. Huang, H. Y. Jia, F. Kajino, K. Kasahara, Y. Katayose, K. Kawata, Labaciren, G. M. Le, J. Y. Li, H. Lu, S. L. Lu, X. R. Meng, K. Mizutani, J. Mu, H. Nanjo, M. Nishizawa, M. Ohnishi, I. Ohta, T. Ouchi, S. Ozawa, J. R. Ren, T. Saito, M. Sakata, T. Sasaki, M. Shibata, A. Shiomi, T. Shirai, H. Sugimoto, K. Taira, M. Takita, Y. H. Tan, N. Tateyama, S. Torii, H. Tsuchiya, S. Udo, T. Utsugi, B. S. Wang, H. Wang, X. Wang, Y. G. Wang, L. Xue, Y. Yamamoto, X. C. Yang, Z. H. Ye, G. C. Yu, A. F. Yuan, T. Yuda, H. M. Zhang, J. L. Zhang, N. J. Zhang, X. Y. Zhang, Y. Zhang, Zhaxisangzhu, and X. X. Zhou, "Absolute Energy Scale Calibration of Multi-TeV Cosmic Rays Using the Moon's Shadow Observed by the Tibet Air Shower Array," in *29th International Cosmic Ray Conference*, vol. 6, 2005, pp. 53–56.

[11] G. Di Sciascio for the ARGO-YBJ collaboration, "Measurements of the angular resolution of the ARGO-YBJ Detector," in *these proceedings*, 2006.

[12] A. . D. v. W. G. V. International Association Of Geomagnetism, S. MacMillan, T. Chernova, S. Choi, D. Dater, V. Golovkov, V. Lesur, F. Lowes, H. Lühr, W. Mai, S. McLean, N. Olsen, M. Rother, T. Sabaka, A. Thomson, and T. Zvereva, "The 10th generation international geomagnetic reference field," *Physics of the Earth and Planetary Interiors*, vol. 151, pp. 320–322, Aug. 2005.

[13] T. K. Gaisser, M. Honda, P. Lipari, and T. Stanev, "Primary spectrum to 1 TeV and beyond," in *27th International Cosmic Ray Conference*, 2001, p. 1643.

[14] P. Vallania, T. Di Girolamo, and C. Vigorito for the ARGO-YBJ collaboration, "First results of the ARGO-YBJ experiment operated in Scaler Mode," in *these proceedings*, 2006.